
000 001 002 003 004 005 IMMUNOTRACE: A META-AGENT FOR IMMUNE HIS- 006 TORY TRACKING 007 008 009

010 **Anonymous authors**
011 Paper under double-blind review
012
013
014
015
016
017
018
019
020
021
022
023
024
025
026
027
028
029
030

ABSTRACT

031 The adaptive immune system encodes an individual’s exposure history in the
032 T-cell receptor (TCR) repertoire. We present **ImmunoTrace**, an AI agent for
033 immune history tracking that estimates past pathogen exposure from a single
034 time-point repertoire by linking TCRs and HLA alleles to proteome-scale pep-
035 tide libraries. A shared protein language model encodes TCR CDR3 sequences,
036 HLA pseudo-sequences, and candidate peptides. Three high-capacity projection
037 heads adapt these embeddings, and two cross-attention modules explicitly model
038 TCR-peptide and HLA-peptide interactions. The fused representation is passed
039 to a deep classifier to produce binding probabilities, while a contrastive branch
040 with an InfoNCE objective and a learnable temperature sculpts the embedding
041 space; we jointly optimize the contrastive and BCE losses while partially fine-
042 tuning ESM2. For subject-level tracking, scores are calibrated into probabili-
043 ties and evidence is aggregated across the repertoire with a probabilistic fusion
044 scheme, yielding pathogen-level exposure estimates together with interpretable
045 peptide-level evidence. On a multi-pathogen benchmark that includes *Treponema*
046 *pallidum* (syphilis) and *Neisseria gonorrhoeae* (gonorrhea), ImmunoTrace sur-
047 passes strong baselines, generalizes under protein and HLA distribution shifts,
048 maintains well-calibrated predictions, and scales to proteome-sized libraries with
049 practical latency. We will release code and data-preparation recipes to facilitate
050 reproducibility.
051
052

1 INTRODUCTION

053 Immunological memory imprints a subject’s exposure history into the T-cell receptor (TCR) reper-
054toire. Each TCR encodes sequence-level constraints that govern recognition of peptide–MHC
055 (pMHC) complexes (Dan et al., 2021). Accurately linking repertoires to peptides across entire
056 pathogen proteomes would enable a new class of computational immunological history trackers that
057 complement serology and nucleic acid tests for routine checkups, diagnosis, vaccine-effectiveness
058 assessment, and personalized therapy. In human syphilis, antigen-specific CD4⁺ T cells in blood
059 and skin persist long after curative therapy (at least 6 months in skin and up to 10 years in blood)
060 and frequently target periplasmic or membrane proteins, underscoring the feasibility of retrospective
061 inference from immune repertoires (Reid et al., 2024).
062

063 Traditional statistical approaches to repertoire analysis—such as k-mer or motif enrichment, public-
064 clonotype lookups, TCR-distance nearest-neighbor classifiers, and pipelines that combine MHC-
065 binding predictors with heuristic TCR features—have yielded useful associations, but they face
066 structural limitations for proteome-scale retrospective inference: (i) they rarely model the full
067 TCR–peptide–MHC triad and cross-reactivity jointly, often omitting the allele sequence or treat-
068 ing it as a coarse label (Montemurro et al., 2021); (ii) they do not naturally scale or calibrate for
069 retrieval over millions of peptides, typically assuming independence across candidates and lacking
070 well-calibrated probabilities; and (iii) they depend on curated epitope labels and immunodominance-
071 biased datasets, limiting generalization to unseen proteins and HLA alleles. These constraints
072 motivate a new AI problem: repertoire-to-proteome linking for retrospective exposure inference (Za-
073 slavsky et al., 2025). Given a single time-point TCR repertoire and optional MHC alleles, and a
074 target pathogen proteome (e.g., *Treponema pallidum* or *Neisseria gonorrhoeae*), the task returns (a)
075 a calibrated subject-level probability of prior exposure and (b) an interpretable, ranked set of candi-
076 date peptides with per-peptide probabilities that support the decision. The formulation emphasizes
077

scalability, calibration, and generalization to unseen proteins and HLA, while aligning with routine clinical workflows.

We introduce ImmunoTrace, an AI agent that orchestrates retrieval, interaction modeling, calibration, and evidence fusion behind a single interface. Concretely, ImmunoTrace: (1) ingests a subject’s single time-point TCR repertoire together with an optional MHC allele sequence; (2) constructs a task-specific peptide library from a target pathogen’s proteome (e.g., *Treponema pallidum*); (3) performs retrieval with a dual-encoder trained using a contrastive objective; (4) performs re-ranking via either a conditional cross-encoder language model that estimates peptide token likelihoods conditioned on (TCR, MHC), or a discriminative interaction module built on a shared protein language model with multi-branch projections and cross-attention; (5) calibrates model scores into probabilities; and (6) aggregates evidence across the repertoire using probabilistic fusion to yield a subject-level exposure probability together with interpretable peptide-level evidence. This decomposition turns a combinatorial search into a scalable two-stage pipeline with calibrated probabilistic output.

Contributions.

- We formalize a **new AI problem**: repertoire-to-proteome linking for retrospective exposure inference, which outputs a calibrated subject-level probability together with an interpretable, ranked set of peptide-level evidence; the formulation targets scalability to proteome-sized libraries and generalization to unseen proteins and HLA alleles.
- We present ImmunoTrace, **an orchestration agent** that combines contrastive retrieval with conditional re-ranking (or a discriminative interaction module), followed by probability calibration and probabilistic fusion, delivering a single end-to-end interface for repertoire-based exposure estimation.
- We establish a **multi-pathogen evaluation** using *Treponema pallidum* (syphilis) and *Neisseria gonorrhoeae* (gonorrhea) as demonstrations, with epitope-level leakage-free splits and out-of-distribution holds (unseen proteins and unseen HLA alleles), release data-preparation recipes, and report strong overall performance with well-calibrated probabilities and practical end-to-end latency.

2 RELATED WORK

We organize prior art along three strands that mirror our pipeline: (i) models of TCR–epitope recognition, which target specificity; (ii) pMHC binding and immunopeptidomics, which constrain peptide availability; and (iii) probability calibration, which turns model scores into repertoire-level, decision-ready outputs.

TCR–epitope prediction. Classical similarity-based methods group receptors by conserved sequence features using alignment or distance metrics (e.g., TCRdist) and motif-oriented clustering (e.g., GLIPH/GLIPH2); they can recover convergent specificity signals but typically do not explicitly model the full TCR–peptide–MHC triad (Dash et al., 2017). Deep models learn joint embeddings for TCRs and peptides (e.g., ERGO, TITAN, DeepTCR, TCRGP, NetTCR, ImRex); some methods incorporate HLA pseudo-sequences or structure-inspired features, yet generalization to unseen epitopes remains challenging (Springer et al., 2020; Weber et al., 2021; Sidhom et al., 2021; Montemurro et al., 2021). Structure-aware resources and methods (e.g., STCRDab-backed pipelines, or docking-and-scoring of TCR–pMHC) can complement sequence-only predictors by providing interface cues and cross-reactivity hypotheses, but they involve throughput trade-offs (Leem et al., 2018; Negi & Braun, 2017). In contrast, our formulation: (a) decouples open-world candidate generation from conditional sequence likelihood by first performing scalable retrieval and then re-ranking; and (b) aggregates pairwise evidence across the entire subject’s repertoire to yield calibrated subject-level probabilities. To ensure fairness in benchmarking and data setup, we reference curated TCR–epitope dictionaries and triad-binding datasets from the Fusion-pMT article and VDJdb, and adapt them into leakage-controlled splits that prevent memorization across TCRs, peptides, or HLA contexts (Ma et al., 2025; Bagaev et al., 2020).

pMHC binding and immunopeptidomics. Predictors such as NetMHCpan and MHCflurry estimate peptide–HLA presentation or binding and are widely used to constrain candidate peptides

108 before any TCR modeling (Reynisson et al., 2020; O’Donnell et al., 2020). Orthogonally, im-
109 munopeptidomics identifies naturally presented ligands by mass spectrometry; public repositories
110 (e.g., PRIDE via ProteomeXchange) and turnkey pipelines (e.g., MHCquant) improve scalability
111 and reproducibility, while rescored frameworks (e.g., MS²Rescore) and multi-engine strategies
112 increase discovery sensitivity in infected-cell ligandomes. In our system, these resources act as
113 optional priors that reduce the retrieval search space without encoding TCR specificity;
114

115 **Calibration.** Accurate downstream use of repertoire-level outputs requires well-calibrated prob-
116 abilities. Post-hoc methods such as Platt scaling, isotonic regression, and temperature scaling are
117 standard tools; temperature scaling in particular is a strong, single-parameter baseline for modern
118 neural networks (Platt et al., 1999; Zadrozny & Elkan, 2002; Guo et al., 2017). We adopt post-
119 hoc calibration on a held-out set and report reliability diagrams, expected calibration error, and
120 probability-accuracy curves at both peptide and subject levels. Practically, calibration stabilizes
121 rule-in/rule-out thresholds for clinical-style readouts. Our focus here is in-distribution calibration;
122 uncertainty quantification under distribution shift is left to future work.

123 3 PRELIMINARIES

124 **Problem setup and notation.** For a subject, let the repertoire be a multiset of TCR sequences
125 with counts, denoted $\mathcal{R} = \{(t_i, c_i)\}_{i=1}^N$, where t_i is a TCR sequence and $c_i \geq 0$ is its clone count
126 (or UMI-derived abundance). We normalize counts into weights $w_i = c_i / \sum_k c_k$ for downstream
127 aggregation. Let m denote an optional MHC pseudo-sequence for the subject; when unavailable
128 we use an uninformative placeholder. Given a pathogen proteome, we form a candidate peptide
129 library $\mathcal{P} = \{p_j\}_{j=1}^M$ by applying variable-length sliding windows at lengths typical for class II
130 presentation (fine stride; details deferred to Methods). The task returns (a) a calibrated subject-level
131 exposure score in $[0, 1]$ and (b) a ranked list of peptide-level evidence items supporting the decision.
132 Unless stated otherwise, overlapping peptides are treated as distinct candidates and no core-based
133 de-duplication is applied.

134 **Sequence representations.** TCRs are represented directly by their amino acid sequences (e.g.,
135 CDR3-centric strings); we do not assume a particular chain configuration in the formulation. Peptides
136 are represented by raw amino acid sequences with variable length. The MHC input is a pseudo-
137 sequence when available; if typing or pseudo-sequences are missing, an uninformative placeholder is
138 used so that the model can condition on MHC when informative but remain robust otherwise. All
139 sequences are tokenized at the residue level and encoded by learned sequence encoders appropriate
140 to each module.

141 **Two-stage scoring.** We adopt a retrieval-then-re-ranking pipeline. A dual-encoder maps (t_i, m)
142 and p_j into a shared embedding space and is trained with an InfoNCE objective so that true pairs
143 have higher similarity than negatives; in practice, in-batch negatives suffice for scalable training:

$$144 \mathcal{L}_{\text{InfoNCE}} = -\log \frac{\exp(\text{sim}(g(t_i, m), h(p_j))/\tau)}{\sum_{p \in \mathcal{N}_i} \exp(\text{sim}(g(t_i, m), h(p))/\tau)},$$

145 where \mathcal{N}_i includes the positive and the in-batch negatives, and τ is a temperature. The re-ranking
146 head is instantiated in two interchangeable forms: (i) a conditional language model that estimates
147 the sequence likelihood of a peptide given (t_i, m) and uses the aggregated token log-likelihood as
148 the score; and (ii) a discriminative cross-encoder that attends over (t_i, m, p_j) jointly and outputs a
149 match score. Either head can be enabled without changing the surrounding pipeline; selection or
150 ensembling strategy is left flexible.

151 **Calibration and repertoire-level fusion.** Pairwise TCR-peptide scores from the re-ranking head
152 are post-hoc calibrated by temperature scaling on a held-out set; in practice, calibration can be ap-
153 plied at the pairwise level and, if desired, again after subject-level fusion. For repertoire-to-subject
154 aggregation we use a simple, frequency-aware, two-level procedure aligned with our implemen-
155 tation. First, for each TCR t_i we score a large batch of candidate peptides and keep its top- K peptide-
156 level evidences (a small constant chosen on a development set). Second, we collect the union of
157 all per-TCR top evidences into a single list of evidence items, each being a pair (t_i, p_j) with its

162 calibrated score; we weight each item by the normalized clone weight w_i , optionally truncate to the
163 top- N items across the subject, and compute a weighted average to obtain the subject-level expo-
164 sure score. Note that evidence aggregation is TCR-first (per-TCR top- K) rather than peptide-first,
165 and identical peptides supported by multiple TCRs are not merged before fusion. Clone-frequency
166 weights are used only at inference-time aggregation; training losses are unweighted.
167

168 4 METHOD

170 4.1 PROBLEM SETUP

172 Given a subject’s TCR repertoire $\mathcal{R} = \{(CDR3_i, count_i)\}_{i=1}^N$, typed MHC allele sequence(s) MHC
173 (covering class I and class II), and a target pathogen proteome \mathcal{G} , our goal is to estimate

$$174 \quad P(\text{exposed} \mid \mathcal{R}, \text{MHC}, \mathcal{G})$$

175

176 and to return the most supportive peptides (and their source proteins) as evidence.
177

178 4.2 AGENT PIPELINE

180 **Algorithm 1** Agent Workflow

181 **Require:** A repertoire–peptide dataset and basic settings
182 1: Set a reproducible seed
183 2: Load and clean the dataset; standardize sequences; remove invalid entries and duplicates
184 3: Build a balanced training set by generating challenging negatives and lightly augmenting posi-
185 tives
186 4: Split by epitope into cross-validation folds to avoid leakage
187 5: **for** each fold **do**
188 6: Initialize a pretrained protein encoder; keep early layers fixed and later layers trainable
189 7: Build a triad model with projections, cross-attention, fusion, a classifier, and a contrastive
190 branch
191 8: Train with mixed precision using a modern optimizer and cosine scheduling; combine clas-
192 sification loss with a gradually weighted contrastive term; apply gradient clipping
193 9: Validate after each epoch; monitor a ranking metric; apply early stopping and keep the best
194 checkpoint
195 10: **end for**
196 11: Aggregate fold results; summarize ranking and classification metrics with bootstrap confidence
197 intervals
198 12: Save checkpoints, logs, plots, and a concise report
199

200 **(1) Peptide library construction.** From each protein in \mathcal{G} we generate a peptide library \mathcal{P} by
201 sliding windows over a small set of lengths suitable for class I and class II presentation. We restrict
202 to canonical amino acids and deduplicate exact peptide strings. No external pMHC pre-filter (e.g.,
203 binding predictors) is used; the downstream retrieval and re-ranking stages learn specificity directly
204 from data. Exact window-length choices and sensitivity analyses are reported in the ablations.

205 **(2) Dual-encoder retrieval.** We build a dual-encoder with parameter sharing across towers. The
206 query tower encodes the pair (CDR3, MHC) using a Transformer encoder; token embeddings are
207 mean-pooled, passed through a linear+ReLU+LayerNorm projection, and ℓ_2 -normalized to obtain
208 $q \in \mathbb{R}^d$. The peptide tower encodes peptide sequences with the same encoder stack and pooling to
209 produce normalized vectors $p \in \mathbb{R}^d$. Training uses an InfoNCE objective with temperature τ :
210

$$211 \quad \mathcal{L}_{\text{InfoNCE}} = -\frac{1}{B} \sum_{i=1}^B \log \frac{\exp(q_i^\top p_i / \tau)}{\sum_{j=1}^B \exp(q_i^\top p_j / \tau)}.$$

212

213 At inference we compute dot products between q and the embedded library matrix and retrieve the
214 top- M candidates per query (approximate nearest-neighbor search is used as needed). Hyperparam-
215 eters d , τ , and M are selected on validation data.

216 (3) **Conditional re-ranking with an autoregressive decoder.** We concatenate the encoder outputs
217 for (CDR3, MHC) as memory and decode peptide tokens with a Transformer decoder trained by
218 teacher-forced negative log-likelihood:

219

$$220 \quad \mathcal{L}_{\text{NLL}} = - \sum_{t=1}^T \log p(y_t | y_{<t}, \text{CDR3}, \text{MHC}).$$

221

222 For each retrieved candidate we compute the average log-likelihood $\ell =$
223 $\frac{1}{T-1} \sum_{t=1}^{T-1} \log p(y_{t+1} | y_{\leq t}, \cdot)$ and use it to re-rank candidates.

224 (4) **Calibration.** We fit a Platt-scaling map on the validation split to convert sequence likelihoods
225 into calibrated compatibility scores, $p = \sigma(a\ell + b)$, and report comparisons to Temperature and
226 Isotonic calibration in the ablations. Calibration is always fit on validation data and never on test.

227 (5) **Two-stage aggregation: protein-level then subject-level.** For each TCR i , we retain up to
228 K highest-probability peptide candidates per source protein g . Let p_{ikg} denote the calibrated com-
229 patibility for TCR i and its k -th kept peptide from protein g ; let $w_i = \frac{\text{count}_i}{\sum_j \text{count}_j}$ be the normalized
230 clonotype weight; and let $\alpha \in (0, 1]$ be a shrinkage factor (selected on validation). Stage 1 (protein-
231 level evidence):

232

$$s_g = 1 - \prod_{i=1}^N \prod_{k=1}^{K_g(i)} (1 - \alpha w_i p_{ikg}),$$

233

234 where $K_g(i) \leq K$ is the number of retained peptides from protein g for TCR i . Stage 2 (subject-
235 level exposure probability):

236

$$P(\text{exposed} | \mathcal{R}, \text{MHC}, \mathcal{G}) = 1 - \prod_{g \in \mathcal{G}} (1 - s_g).$$

237

238 4.3 TRAINING DATA AND NEGATIVES

239 We assemble triples (CDR3, MHC, peptide) from public resources (e.g., VDJdb, McPAS-TCR,
240 IEDB) and construct leakage-controlled splits at the *epitope* level, with additional protein-level out-
241 of-distribution holds. Negatives are formed by a $10\times$ expansion per positive: (i) length-matched
242 peptides sampled from the same pool and (ii) point-mutated variants with 1–2 substitutions. The
243 negative ratio, embedding dimension, calibration type, and other design choices are ablated (see the
244 ablation results), while the main results use the defaults stated above.

245 5 EXPERIENCE

246 5.1 BASELINE COMPARISON

247 Figure 1a reports ROC AUC for a representative set of baselines under a unified data split and eval-
248 uation protocol. The panel includes classical feature- or similarity-based methods (K-mer, Logistic,
249 Random Forest, TCRdist ($k=5$)), a presentation-only reference (MHCflurry), pretrained representa-
250 tion learning approaches (ProtBert, GNN). To ensure fair comparison and guard against memoriza-
251 tion, we employ leakage-controlled, epitope-level splits and evaluate under protein- and HLA-shift
252 holds with identical candidate libraries and search spaces across models.

253 We observe the following trends:

254

- 255 • **Representation learning and interaction modeling** generally outperform hand-crafted
256 features and distance-based methods, underscoring the importance of shared sequence em-
257 beddings for repertoire-to-proteome retrieval.
- 258 • **MHCflurry as a lower-bound reference:** it constrains peptide presentation but does not
259 model TCR specificity, making it useful for pruning the candidate space yet limited as a
260 standalone predictor for TCR–peptide recognition.

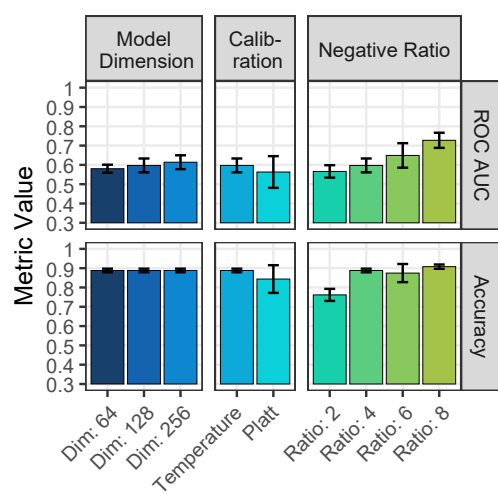
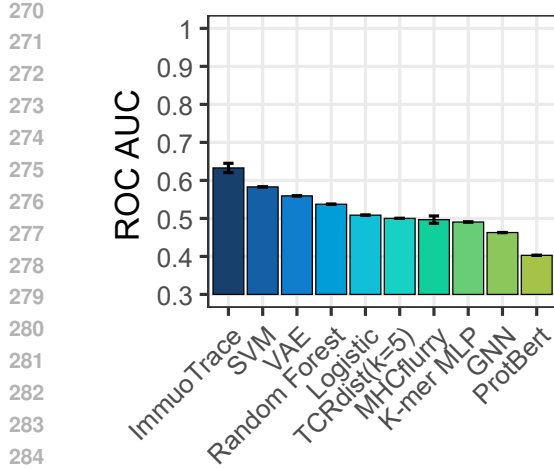


Figure 1: Main Results. (a) Baseline comparison; (b) Ablation studies

- **Pretrained LMs and neural baselines** (e.g., ProtBert, GNN) are competitive; however, the retrieval–then–re-ranking pipeline tends to be more robust under HLA and protein distribution shifts while scaling to proteome-sized libraries.
- **ImmunoTrace** ranks among the top performers and often achieves the best ROC AUC, suggesting that contrastive retrieval combined with conditional re-ranking and post-hoc calibration is advantageous for calibrated, large-scale peptide retrieval.

5.2 ABLATION STUDIES

Figure 1b presents ablations over three design factors and their impact on ROC AUC and Accuracy: (i) embedding dimension (64/128/256), (ii) probability calibration method (Temperature vs. Platt), and (iii) the negative-to-positive ratio used in contrastive training (2/4/6/8). Key findings are:

Embedding dimension. Increasing from 64 to 128 yields a clear improvement, while moving from 128 to 256 provides smaller, diminishing gains. Considering memory and latency, $Dim=128$ offers a strong accuracy–efficiency trade-off.

Calibration. Both Temperature scaling and Platt scaling improve thresholded Accuracy without materially altering ranking quality (AUC), consistent with their role as post-hoc calibration methods. Temperature scaling, with a single parameter, exhibits more stable behavior across splits and is adopted as our default. Reliability diagrams and ECE metrics are reported in the appendix.

Negative ratio. Raising the negative ratio from 2 to 6 steadily improves both AUC and Accuracy, reflecting a sharper contrastive boundary and higher-quality retrieval. Further increasing to 8 yields marginal gains at higher computational cost, indicating diminishing returns.

5.3 CASE STUDIES AND DEMO

We demonstrate an end-to-end run for *Treponema pallidum* (syphilis) using the proposed retrieval + re-ranking pipeline. The subject-level output reports: Risk Category: Low Risk; Exposure Score: 0.041 (4.1%); Evidence Count: 20. All entries are conditioned on the same MHC pseudo-sequence: QEFFIASGAAVDAIMWLFLEYDLQRATYHVGFT. A compact subset of the Top-15 TCR–peptide evidence items is shown in Table 1; the full ranked list remains in the appendix.

324 Table 1: Top TCR–Peptide Binding Evidence for Syphilis (compact subset of Top-15 and list Top-8
325 here for illustration).

Rank	TCR (CDR3)	Pathogen Peptide	Binding Score
1	CASSGTGGYEQYF	SLCVRLTPG	0.813
2	CASSGTGGYEQYF	LSEHLRSCE	0.813
3	CASSGTGGYEQYF	SLVGERLTL	0.812
4	CASSERTSGGRDTQYF	SLCVRLTPG	0.812
5	CASSERTSGGRDTQYF	LSEHLRSCE	0.811
6	CASSGTGGYEQYF	FETPREVEV	0.811
7	CASSERTSGGRDTQYF	SLVGERLTL	0.811
8	CASSLRIAGGPDTQYF	SLCVRLTPG	0.811

335

336

337

6 DISCUSSION AND BROADER IMPACT

340 **Scientific implications.** Our method (ImmunoTrace) offers a computational and AI perspective
341 to read out signals of immunological exposure from TCR repertoires, complementing serology and
342 PCR tests. The retrieval + re-ranking decomposition is modular and can incorporate structural priors,
343 peptide–MHC (pMHC) predictors, and mass-spectrometry–eluted ligand catalogs, enabling contin-
344 ued integration of external knowledge without altering the overall framework.

345

346

347 **Limitations.** The approach relies on the availability and representativeness of paired TCR–peptide
348 data. Probability calibration depends on the validation distribution; cross-cohort distribution shift
349 may require re-calibration. Peptides generated by sliding windows only approximate antigen pre-
350 sentation and do not guarantee immunogenicity. Accordingly, outputs should be interpreted with
351 appropriate biological prior knowledge and, where applicable, supported by clinical validation.

352

353 **Future Directions** We see several avenues for advancing this line of work: - Prospective, multi-
354 center evaluations with pre-registered protocols; cohort-shift-aware calibration (e.g., domain adap-
355 tation, conformal risk control) for reliable deployment across sites. - Richer antigen-processing
356 priors beyond sliding windows, integrating cleavage/transport models, HLA class–specific binding,
357 and MS-eluted ligand evidence; systematic analyses of overlapping peptides and core-based con-
358 solidation. - Improved biological conditioning, including explicit TCR α/β pairing when available,
359 gene-usage features, and refined MHC inputs; ablations of peptide-first versus TCR-first evidence
360 aggregation(Tanno et al., 2020). - Safety and privacy: model cards, responsible-use licensing,
361 optional privacy-preserving training (e.g., federated or differentially private variants), and continuous
362 monitoring for distribution shift and potential misuse. - Scalability: faster approximate nearest-
363 neighbor indexing, product quantization, and batching strategies to support proteome-scale and
364 multi-pathogen libraries without sacrificing calibration quality.

365

366

367

7 CONCLUSION

368

369 We presented *ImmunoTrace*, a meta-agent that reconstructs immune exposure history from a single
370 time-point T-cell receptor (TCR) repertoire by linking TCRs and HLA alleles to proteome-scale pep-
371 tide libraries. The system combines a shared protein language model with high-capacity projections
372 and dual cross-attention to model TCR–peptide and HLA–peptide interactions. A retrieval–then–re-
373 ranking workflow trained with a contrastive InfoNCE objective enables scalable candidate genera-
374 tion, while post-hoc calibration and probabilistic fusion aggregate evidence across the repertoire to
375 yield a calibrated, subject-level exposure probability together with interpretable peptide-level sup-
376 port. ImmunoTrace catalyzes a new class of retrieval-augmented, repertoire-to-proteome tools that
377 provide calibrated, interpretable readouts of immune history and complement existing serological
and nucleic-acid assays.

378 **BIOSAFETY AND MISUSE STATEMENT**

379

380 We recognize the dual-use nature of immune modeling. This work must not be used to design
381 immune-evasive peptides, to enhance pathogen properties, or to conduct activities that increase bio-
382 logical risk. To mitigate misuse, we will: (i) release only de-identified data and scripts to reconstruct
383 public datasets; (ii) adopt a research-and-education license and terms of use that explicitly prohibit
384 applications aimed at immune evasion, gain-of-function, or other harmful purposes; (iii) avoid re-
385 leasing precomputed, proteome-wide ranked peptide lists for high-risk organisms; (iv) document
386 model limitations and uncertainty to reduce overinterpretation; and (v) encourage responsible dis-
387 closure and community oversight. Any experimental use must comply with applicable biosafety
388 regulations (e.g., appropriate BSL containment) and institutional approvals.

389

390 **ETHICS STATEMENT**

391

392 All datasets are public and de-identified; license terms are respected. The system is intended for
393 research and educational purposes and not for clinical diagnosis. Any prospective clinical use would
394 require Institutional Review Board (IRB) approval, informed consent, and rigorous pre-deployment
395 validation.

396

397 **THE USE OF LLMs**

398

399 We acknowledge the use of large language models, specifically OpenAI GPT-5, to improve the
400 clarity, grammar, and stylistic consistency of the manuscript, and to help standardize mathematical
401 notation and LaTeX equation formatting. We also used text-to-image generative models to draft and
402 refine schematic illustrations; all figures were curated and finalized by the authors. AI tools were
403 not used for data collection, analysis, experiment design, or for generating scientific claims. The
404 authors independently verified all outputs and take full responsibility for any remaining errors. Only
405 non-sensitive manuscript text and high-level figure descriptions were provided to these tools.

406

407 **REFERENCES**

408 Dmitry V Bagaev, Renske MA Vroomans, Jerome Samir, Ulrik Stervbo, Cristina Rius, Garry
409 Dolton, Alexander Greenshields-Watson, Meriem Attaf, Evgeny S Egorov, Ivan V Zvyagin, et al.
410 Vdjdb in 2019: database extension, new analysis infrastructure and a t-cell receptor motif com-
411 pendium. *Nucleic acids research*, 48(D1):D1057–D1062, 2020.

412 Jennifer M Dan, Jose Mateus, Yu Kato, Kathryn M Hastie, Esther Dawen Yu, Caterina E Faliti,
413 Alba Grifoni, Sydney I Ramirez, Sonya Haupt, April Frazier, et al. Immunological memory to
414 sars-cov-2 assessed for up to 8 months after infection. *Science*, 371(6529):eabf4063, 2021.

415

416 Pradyot Dash, Andrew J Fiore-Gartland, Tomer Hertz, George C Wang, Shalini Sharma, Aisha
417 Souquette, Jeremy Chase Crawford, E Bridie Clemens, Thi HO Nguyen, Katherine Kedzierska,
418 et al. Quantifiable predictive features define epitope-specific t cell receptor repertoires. *Nature*,
419 547(7661):89–93, 2017.

420 Chuan Guo, Geoff Pleiss, Yu Sun, and Kilian Q Weinberger. On calibration of modern neural
421 networks. In *International conference on machine learning*, pp. 1321–1330. PMLR, 2017.

422

423 Jinwoo Leem, Saulo H P de Oliveira, Konrad Krawczyk, and Charlotte M Deane. Stcrdb: the
424 structural t-cell receptor database. *Nucleic acids research*, 46(D1):D406–D412, 2018.

425

426 Jiahao Ma, Hongzong Li, Jian-Dong Huang, Ye-Fan Hu, and Yifan Chen. Remodeling peptide-
427 mhc-tcr triad binding as sequence fusion for immunogenicity prediction. *arXiv preprint*
428 arXiv:2501.01768, 2025.

429

430 Alessandro Montemurro, Viktoria Schuster, Helle Rus Povlsen, Amalie Kai Bentzen, Vanessa Jurtz,
431 William D Chronister, Austin Crinklaw, Sine R Hadrup, Ole Winther, Bjoern Peters, et al. Nettcr-
2.0 enables accurate prediction of tcr-peptide binding by using paired tcr α and β sequence data.
432 *Communications biology*, 4(1):1060, 2021.

432 Surendra S Negi and Werner Braun. Cross-react: a new structural bioinformatics method for pre-
433 dicting allergen cross-reactivity. *Bioinformatics*, 33(7):1014–1020, 2017.
434

435 Timothy J O'Donnell, Alex Rubinsteyn, and Uri Laserson. Mhcflurry 2.0: improved pan-allele
436 prediction of mhc class i-presented peptides by incorporating antigen processing. *Cell systems*,
437 11(1):42–48, 2020.

438 John Platt et al. Probabilistic outputs for support vector machines and comparisons to regularized
439 likelihood methods. *Advances in large margin classifiers*, 10(3):61–74, 1999.
440

441 Tara B Reid, Charmie Godornes, Victoria L Campbell, Kerry J Laing, Lauren C Tantalo, Alloysius
442 Gomez, Thepthona N Pholsena, Nicole AP Lieberman, Taylor M Krause, Victoria I Cegielski,
443 et al. *Treponema pallidum* periplasmic and membrane proteins are recognized by circulating and
444 skin cd4+ t cells. *The Journal of Infectious Diseases*, 230(2):281–292, 2024.

445 Birkir Reynisson, Bruno Alvarez, Sinu Paul, Bjoern Peters, and Morten Nielsen. Netmhcpant-4.1
446 and netmhciipan-4.0: improved predictions of mhc antigen presentation by concurrent motif de-
447 convolution and integration of ms mhc eluted ligand data. *Nucleic acids research*, 48(W1):W449–
448 W454, 2020.

449 John-William Sidhom, H Benjamin Larman, Drew M Pardoll, and Alexander S Baras. Deeptrc
450 is a deep learning framework for revealing sequence concepts within t-cell repertoires. *Nature
451 communications*, 12(1):1605, 2021.
452

453 Ido Springer, Hanan Besser, Nili Tickotsky-Moskovitz, Shirit Dvorkin, and Yoram Louzoun. Pre-
454 diction of specific tcr-peptide binding from large dictionaries of tcr-peptide pairs. *Frontiers in
455 immunology*, 11:1803, 2020.

456 Hidetaka Tanno, Timothy M Gould, Jonathan R McDaniel, Wenqiang Cao, Yuri Tanno, Russell E
457 Durrett, Daechan Park, Steven J Cate, William H Hildebrand, Cornelia L Dekker, et al. Determinants
458 governing t cell receptor α/β -chain pairing in repertoire formation of identical twins.
459 *Proceedings of the National Academy of Sciences*, 117(1):532–540, 2020.

460 Anna Weber, Jannis Born, and María Rodriguez Martínez. Titan: T-cell receptor specificity predic-
461 tion with bimodal attention networks. *Bioinformatics*, 37(Supplement_1):i237–i244, 2021.
462

463 Bianca Zadrozny and Charles Elkan. Transforming classifier scores into accurate multiclass proba-
464 bility estimates. In *Proceedings of the eighth ACM SIGKDD international conference on Knowl-
465 edge discovery and data mining*, pp. 694–699, 2002.

466 Maxim E Zaslavsky, Erin Craig, Jackson K Michuda, Nidhi Sehgal, Nikhil Ram-Mohan, Ji-Yeun
467 Lee, Khoa D Nguyen, Ramona A Hoh, Tho D Pham, Katharina Röltgen, et al. Disease diagnostics
468 using machine learning of b cell and t cell receptor sequences. *Science*, 387(6736):eadp2407,
469 2025.
470

471

472

473

474

475

476

477

478

479

480

481

482

483

484

485

486 A PATHOGEN-SPECIFIC IMMUNITY REPORTS 487

488 This appendix presents two subject-level immunity analyses produced by our retrieval + re-ranking
489 pipeline. Each report includes a risk category, Exposure Score, evidence count, held-out model
490 performance (AUC, Accuracy), and the Top-15 TCR-peptide binding evidence items that support
491 interpretation. These outputs are for research and education only and are not clinical diagnostics.
492 To reduce misuse risk, we show only the Top-15 evidence items; full ranked lists for high-risk
493 organisms are not released.

494 495 A.1 SYPHILIS (TREPONEMA PALLIDUM) 496

497 **Summary.** Risk Category: Low Risk; Exposure Score: 0.041 (4.1%); Evidence Count: 20.
498 Model AUC: 0.753; Model Accuracy: 0.745.

499 All entries are conditioned on the same MHC pseudo-sequence input:
500 QEFFIASGAAVDAIMWLFLCYDLQRATYHVGFT.

501
502 **Narrative.** The Top-15 evidence shows multiple motif-sharing TCRs (CASSGTGGYEQYF,
503 CASSERTSGGRDTQYF, CASSLRIAGGPDTQYF) matching several candidate peptides
504 (SLCVRLTPG, LSEHLSCE, SLVGERLTL, FETPREVEV, SARPKHITV, FVASQMTDAR)
505 with closely clustered scores (0.807–0.813). In conjunction with the 4.1% Exposure Score and
506 held-out performance, this pattern supports a Low Risk assessment for the current sample.

507 508 A.2 GONORRHEA (NEISSERIA GONORRHOEAE)

509
510 **Summary.** Risk Category: Low Risk; Exposure Score: 0.040 (4.0%); Evidence Count: 20.
511 Model AUC: 0.753; Model Accuracy: 0.745.

512 All entries are conditioned on the same MHC pseudo-sequence input:
513 QEFFIASGAAVDAIMWLFLCYDLQRATYHVGFT.

514
515 **Narrative.** For gonorrhea, peptides such as TLRRSGLFEA and SQDVVVRLL recur
516 across multiple TCRs (CASSGTGGYEQYF, CASSERTSGGRDTQYF, CASSLRIAGGPDTQYF,
517 CASSLSGAYEQYF) with scores in the 0.806–0.815 range. Together with the 4.0% Exposure Score
518 and model-level performance, this pattern indicates a Low Risk exposure signal for the sample.

519
520 **Safety and Misuse Note.** These appendix lists are provided solely for reproducibility and scholarly
521 discussion. They must not be used to design immune-evasive sequences or for any activity that
522 increases biological risk. Any redistribution or downstream use must comply with project licensing,
523 institutional review, and applicable laws and biosafety regulations.

524
525 Table 2: Top TCR–Peptide Binding Evidence for Syphilis (Top-15).
526

527 Rank	528 TCR (CDR3)	529 Pathogen Peptide	530 Binding Score
1	CASSGTGGYEQYF	SLCVRLTPG	0.813
2	CASSGTGGYEQYF	LSEHLSCE	0.813
3	CASSGTGGYEQYF	SLVGERLTL	0.812
4	CASSERTSGGRDTQYF	SLCVRLTPG	0.812
5	CASSERTSGGRDTQYF	LSEHLSCE	0.811
6	CASSGTGGYEQYF	FETPREVEV	0.811
7	CASSERTSGGRDTQYF	SLVGERLTL	0.811
8	CASSLRIAGGPDTQYF	SLCVRLTPG	0.811
9	CASSLRIAGGPDTQYF	LSEHLSCE	0.810
10	CASSGTGGYEQYF	SARPKHITV	0.810
11	CASSERTSGGRDTQYF	FETPREVEV	0.810
12	CASSLRIAGGPDTQYF	SLVGERLTL	0.810
13	CASSERTSGGRDTQYF	SARPKHITV	0.808
14	CASSLRIAGGPDTQYF	FETPREVEV	0.808
15	CASSLRIAGGPDTQYF	FVASQMTDAR	0.807

540 Table 3: Top TCR–Peptide Binding Evidence for Gonorrhea (Top-15).
 541

Rank	TCR (CDR3)	Pathogen Peptide	Binding Score
1	CASSGTGGYEQYF	TLRRSGLFEA	0.815
2	CASSGTGGYEQYF	SQDVVVRLLRT	0.815
3	CASSERTSGGRDTQYF	TLRRSGLFEA	0.814
4	CASSERTSGGRDTQYF	SQDVVVRLLRT	0.813
5	CASSLRIAGGPDTQYF	TLRRSGLFEA	0.813
6	CASSLRIAGGPDTQYF	SQDVVVRLLRT	0.812
7	CASSGTGGYEQYF	STSTAHLG	0.809
8	CASSLSGAYEQYF	TLRRSGLFEA	0.809
9	CASSLSGAYEQYF	SQDVVVRLLRT	0.808
10	CASSGTGGYEQYF	TTFPTYFELE	0.808
11	CASSERTSGGRDTQYF	STSTAHLG	0.808
12	CASSGTGGYEQYF	FTSRYIFAT	0.808
13	CASSERTSGGRDTQYF	FTSRYIFAT	0.807
14	CASSLRIAGGPDTQYF	STSTAHLG	0.806
15	CASSERTSGGRDTQYF	TTFPTYFELE	0.806

556
 557 **B INTERPRETING IMMUNE HISTORY FROM TCR REPERTOIRES:**
 558 **BIOLOGICAL BASIS AND APPLICATIONS**
 559

560 **B.1 WHAT DOES A TCR REPERTOIRE ENCODE ABOUT IMMUNE HISTORY?**
 561

562 The T-cell receptor (TCR) repertoire is generated by somatic V(D)J recombination and diversified by
 563 imprecise junctional processes (e.g., N-nucleotide addition) followed by thymic selection, yielding a
 564 vast, individualized set of clonotypes.¹ Upon infection or vaccination, antigen-specific naive T cells
 565 undergo clonal expansion, contraction, and transition into long-lived memory subsets (e.g., T_{CM},
 566 T_{EM}, T_{EMRA}, T_{SCM}). Immunological memory at the organism level can persist for years to decades,
 567 even though individual memory T cells are dynamically maintained with subset-dependent turnover.
 568 These dynamics leave measurable, sequence-level imprints of past antigen encounters in blood and
 569 tissues, which can be read out by repertoire sequencing and computational modeling.
 570

571 **B.2 ANTIGEN PROCESSING, PRESENTATION, AND WHY PEPTIDE CONTEXT MATTERS**
 572

573 TCRs recognize peptides presented by MHC molecules. MHC-I typically presents proteasome-
 574 derived intracellular peptides to CD8⁺ T cells; MHC-II presents endosomal/exogenous peptides
 575 to CD4⁺ T cells, with cross-presentation and autophagy providing additional crosstalk. The im-
 576 munopeptidome depends on source-protein abundance, turnover, processing, and MHC binding
 577 motifs. Modern in silico predictors (e.g., NetMHCpan families) trained on binding and MS-eluted
 578 ligands, and immunopeptidomics by mass spectrometry, provide priors on which peptides are likely
 579 presented in vivo. For exposure inference, these priors constrain the peptide search space and inform
 580 the retrieval step, while downstream re-ranking integrates sequence-level evidence from candidate
 581 pMHCs and observed TCRs.
 582

583 **B.3 SPECIFICITY, CROSS-REACTIVITY, AND IMMUNODOMINANCE**
 584

585 TCR specificity is degenerate: most TCRs recognize sets of related pMHCs because binding of-
 586 ten focuses on a limited number of peptide-facing residues and allows structural plasticity at the
 587 pMHC interface. Cross-reactivity underpins coverage of the astronomical epitope universe with a
 588 finite repertoire, but also complicates exposure readouts by introducing heterologous recognition.
 589 Prior infections can reshape immunodominance hierarchies, producing oligoclonal boosts of cross-
 590 reactive clones; in extreme cases, this facilitates pathogen escape or immunopathology. Structural
 591 mimicry between self and pathogen peptides further explains links between infection history and
 592 autoimmunity. For repertoire-based exposure models, these principles motivate conservative cali-
 593 bration, pathogen panel design, and cross-pathogen negative controls.
 594

595 ¹Key terms: clonotype (cells sharing essentially identical TCR CDR3), public vs. private TCRs (widely
 596 shared vs. individual-specific), generation probability P_{gen} (likelihood that recombination produces a given
 597 sequence).

594 B.4 PUBLIC AND PRIVATE TCRs, HLA INFLUENCES, AND WHAT IS LEARNABLE ACROSS
595 PEOPLE
596

597 Widely shared (“public”) TCRs arise in part from convergent recombination and selection bi-
598 ases, whereas most responding TCRs remain “private.” Generation probability and thymic selection
599 jointly predict the degree of sharing in cohorts. Large-cohort immunosequencing has demonstrated
600 that exposure to common pathogens (e.g., CMV) imprints reproducible sequence signatures suf-
601 ficient to classify serostatus and even infer HLA restrictions. However, HLA polymorphism also
602 sculpts the effective antigenic space per person, influencing which TCRs are positively selected
603 and boosted during life. Inference pipelines benefit from modeling: (i) cohort-level public signals,
604 (ii) subject-specific private expansions, and (iii) HLA conditioning (genotyped or approximated via
605 pseudo-sequences).

606 B.5 FROM SEQUENCES TO EXPOSURE READOUTS: PRACTICAL INTERPRETATION
607

608 When inferring exposure history:

- 610 • Use consistent sampling (blood volume, cell subset), bias-controlled library construction,
611 and depth sufficient to detect expanded memory clones; quantify clonality and diversity to
612 contextualize findings.
- 613 • Condition retrieval on plausible pMHCs (MHC allele set, proteome, processing priors)
614 and report uncertainty; prefer peptide panels with immunopeptidomic or literature support
615 when available.
- 616 • Aggregate evidence at the repertoire level (e.g., weighted by clone size) and calibrate on
617 validation distributions; provide observer-operating points (ROC/AUPRC) and reliability
618 diagnostics (ECE, calibration plots).
- 619 • Treat outputs as probabilistic exposure signals, not clinical diagnoses; triangulate with
620 serology/PCR, clinical history, and—where relevant—functional assays (e.g., ELISpot,
621 tetramers).

623 B.6 CONFOUNDERS AND RECOMMENDED CONTROLS
624

625 Repertoire readouts can be confounded by:

- 626 • **Bystander activation and homeostatic proliferation:** cytokine-driven expansions with-
627 out cognate antigen engagement may transiently elevate unrelated clones.
- 628 • **Microbiome-driven cross-reactivity:** commensal peptides can prime cross-reactive T
629 cells that respond to tumor or pathogen epitopes.
- 630 • **Sampling and technical factors:** depth, chain pairing (unpaired α/β), tissue compartmen-
631 talization, batch effects; mitigate via replicate libraries, UMI strategies, and, when possible,
632 paired-chain single-cell data.
- 633 • **HLA uncertainty:** unavailable genotypes necessitate assumptions or imputation; report
634 the assumed allele set and perform sensitivity analyses.

636 Recommended controls include cross-pathogen decoys, longitudinal baselines, cohort-shift-aware
637 recalibration, and prospective preregistration of operating thresholds.

639 B.7 APPLICATIONS: WHERE REPERTOIRE-ENCODED IMMUNE HISTORY HELPS
640

641 **Infectious diseases.** Population studies show TCR signatures can retrospectively classify expo-
642 sures (e.g., CMV), complementing serology—especially when antibodies wane or in immunocom-
643 promised hosts. Longitudinal profiling tracks post-infection contraction and memory stabilization
644 and can reveal pre-existing cross-reactive memory.

645 **Vaccination.** Repertoire tracking quantifies vaccine-responding clones, convergence across in-
646 dividuals, and durability by subset. In trials, TCR analytics can benchmark immunodominance
647 breadth, HLA coverage, and dose/schedule effects beyond antibody titers.

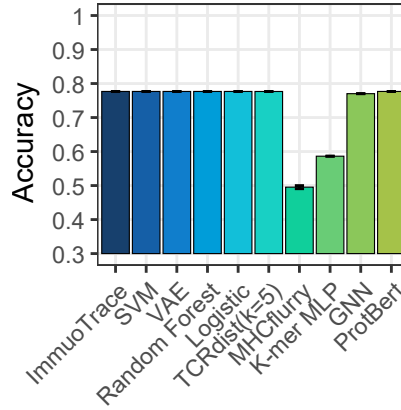
648
649 **Transplantation and immunosuppression.** Pathogen-specific T-cell monitoring (e.g., CMV) im-
650 proves risk stratification relative to serostatus alone and guides prophylaxis windows.

651 **Oncology and autoimmunity.** In tumors, TCR-seq supports minimal residual disease track-
652 ing, TIL clonality assessment, and response prediction for checkpoint blockade; in autoimmunity,
653 disease-relevant TCRs (e.g., insulin-reactive) can serve as mechanistic biomarkers. Cross-reactivity
654 and tissue compartmentalization require careful interpretation and validation.

655 **B.8 SCOPE, BIOSAFETY, AND RESPONSIBLE USE**

656 Repertoire-based exposure inference is intended for research and surveillance, not standalone di-
657 agnosis. Analyses must avoid designing immune-evasive peptides or publishing exhaustive high-
658 risk epitope rankings. Data sharing should prioritize de-identified repertoires and controlled-access
659 metadata, with IRB/ethics compliance for any prospective clinical deployment.

660 **C APPENDIX COMPREHENSIVE BASELINE ACCURACY**



661
662 Figure 2: Comprehensive baseline comparison (Accuracy). Models: ImmunoTraceSVMVAE, Ran-
663 dom Forest, Logistic, TCRdist (k=5), MHCflurry, K-mer, MLPGNN, ProtBert.

664
665 Figure 2 complements the main ROC AUC results by reporting thresholded Accuracy for the same
666 set of baselines under an identical data split and evaluation protocol. Accuracy summarizes decision
667 performance at a fixed operating point and is thus informative for downstream deployment scenarios
668 where a single threshold is required.

669 **Evaluation protocol.** 1. **Unit of evaluation.** Pairwise TCR-peptide recognition on the
670 leakage-controlled, epitope-level test set; protein- and HLA-shift holds follow the same protocol.
671 All methods score the identical candidate peptide libraries. 2. **Calibration.** For each model, scores
672 are post-hoc calibrated on the validation split via temperature scaling, yielding probabilities in [0, 1]
673 without altering ranking. 3. **Operating threshold.** Unless otherwise noted, we apply a fixed thresh-
674 old of 0.5 to calibrated probabilities on the test set. Results using validation-selected thresholds (e.g.,
675 maximizing balanced accuracy or Youden's J) exhibit consistent trends and are provided in the code
676 release. 4. **Class balance.** The test-set positive/negative ratio is preserved from data preparation; for
677 completeness, we also compute balanced accuracy and per-class metrics (reported in supplementary
678 tables).

679 **Key observations.** 1. **Representation learning and interaction modeling** (ProtBert, MLPGNN,
680 and especially our ImmunoTrace variant) generally achieve higher Accuracy than hand-crafted or
681 distance-based baselines (K-mer, Logistic, Random Forest, TCRdist (k=5)), mirroring the ROC
682 AUC ordering in the main text. 2. **MHCflurry** provides a useful presentation prior but lacks TCR
683 specificity; as a standalone classifier, its Accuracy trails methods that model TCR-peptide interac-
684 tions. 3. **ImmunoTrace (ImmunoTraceSVMVAE)** remains among the top performers in Accuracy,

702 indicating that contrastive retrieval plus conditional re-ranking and post-hoc calibration translate
703 into superior decision-level performance at fixed thresholds. 4. The **relative ranking** is stable
704 across in-distribution and shift settings (unseen proteins and unseen HLA), suggesting robustness of
705 the retrieval+re-ranking pipeline to distributional variation.

706
707 **Robustness checks.** 1. **Threshold sensitivity.** Using validation-optimized thresholds (balanced
708 accuracy or Youden’s J) yields the same qualitative ordering of methods. 2. **Class imbalance.**
709 Balanced accuracy and per-class precision/recall align with the Accuracy trends, mitigating concerns
710 that improvements stem from prevalence alone. 3. **Shift analysis.** Under protein- and HLA-shift
711 holds, Accuracy degrades uniformly across models, but the gap between interaction-aware methods
712 and simpler baselines persists.

713
714 **D TRAINING AND IMPLEMENTATION DETAILS**

715
716 We trained the system in Python 3.10 using PyTorch, HuggingFace Transformers and Accelerate,
717 scikit-learn, NumPy/Pandas, and Matplotlib/Seaborn on a single CUDA device with bf16
718 mixed precision and a global seed of 42; the sequence encoder is ESM2 (12-layer, \sim 35M
719 parameters) shared across TCR CDR3 (primarily β -chain), typed MHC class I/II amino acid se-
720 quences, and peptides, using the `[CLS]` token as the sequence embedding, freezing only the first
721 two transformer layers while keeping embeddings and the pooler trainable, projecting each stream
722 through two FC+LayerNorm+GELU blocks to d dimensions (default $d=128$ with ablations over
723 $\{64, 128, 256\}$), applying multi-head cross-attention between (TCR, peptide) and (MHC, peptide)
724 followed by a multi-layer fusion MLP and a BCE-with-logits classifier head augmented with an
725 InfoNCE branch whose weight ramps from 0.1 to 0.5 over epochs with a learnable temperature
726 initialized at 0.07; optimization uses AdamW with parameter-wise learning rates (ESM par-
727 ameters at $0.05\times$ the base rate, attention/fusion at $0.5\times$, others at the base rate), weight decay of
728 $0.01/0.05/0.10$ for ESM/attention/projection parameter groups, cosine annealing with warm restarts
729 ($T_0=\lfloor \text{epochs}/3 \rfloor$, $T_{\text{mult}}=2$, $\eta_{\text{min}}=10^{-7}$), gradient clipping at 1.0, gradient accumulation of 2, batch
730 size 64, 10 epochs, base learning rate 10^{-4} , and early stopping on validation AUC with patience 8;
731 calibration uses Platt scaling on the validation split, with ablations comparing temperature and iso-
732 tonic calibration; retrieval relies solely on sliding-window peptide libraries over pathogen proteomes
733 without pMHC pre-filtering, a shared-parameter dual encoder with mean pooling to embed query
734 pairs (CDR3+MHC) and peptides, and re-ranking via an autoregressive decoder scored by average
735 log-likelihood, while the number of retrieved candidates (top- M), the per-TCR keep count K , and
736 the aggregation shrinkage factor α are selected on validation; negatives are constructed at roughly
737 $10\times$ per positive via length-matched random peptides, 1–3 position point mutations, and cross-MHC
738 mismatches, followed by deduplication and optional positive augmentation to approach class bal-
739 ance (a representative run after balancing yields a positive:negative ratio of about 1.9:1 with minor
740 fold-to-fold variability); data splits enforce five-fold cross-validation at the epitope level to prevent
741 leakage (train/validation/test epitopes are disjoint), training and evaluation are logged per epoch with
742 cross-validation summaries, and the best checkpoint is restored by loading the saved state dict on
743 the unwrapped model when distributed wrappers are used; hyperparameter ranges for embedding
744 dimension, calibration choice, and negative ratios are explored in ablations.

745
746
747
748
749
750
751
752
753
754
755